Evaluation of Physical Properties and Image of Polyvinyl Chloride as Breast Tissue Equivalence for Dual-Modality (Mammography and Ultrasound)

Aditya Prayugo Hariyanto
Institut Teknologi Sepuluh Nopember Fakultas Sains dan Analitika Data
Nurhanifa Tri Budiarti
Gambiran General Hospital Kediri
Suprijanto Suprijanto
Institut Teknologi Bandung Fakultas Teknik Industri
Kwan Hoong Ng
University of Malaya Faculty of Medicine
Freddy Haryanto
Institut Teknologi Bandung Fakultas Matematika dan Ilmu Pengetahuan Alam
Endarko Endarko (endarko@physics.its.ac.id)
Institut Teknologi Sepuluh Nopember Fakultas Sains dan Analitika Data https://orcid.org/0000-0001-8238-1983

Research Article

Keywords: polyvinyl chloride, tissue mimicking, attenuation, the speed of sound, dual-modality

Posted Date: December 9th, 2022

DOI: https://doi.org/10.21203/rs.3.rs-2351981/v1

Abstract

Tissue-mimicking phantom (TMP) is gradually becoming a fundamental element for quality assurance and control in ionizing and non-ionizing radiation imaging modalities as well as in the development of different techniques. This study aims to evaluate polyvinyl chloride (PVC) tissue mimicking material for dual-modality breast phantoms in mammography and ultrasound. Breast tissue equivalence was evaluated based on X-ray attenuation properties, speed of sound, attenuation, and acoustic impedance. There are six samples of PVC-plasticizer material with variations of PVC concentration and additives. The evaluation of X-ray attenuation was carried out using mammography from 23–35 kV, while the acoustic properties were assessed with mode A ultrasound and a transducer frequency of 5 MHz. A breast phantom was created from TMP material with tissue equivalence and was evaluated using mammography as well as ultrasound to analyze its image quality. The results showed that samples A, B, C, E, and F have the closest equivalent to the ACR breast phantom material with a different range of 0.01–1.39 in the 23–35 kV range. Based on the evaluation of the acoustic properties of ultrasound, A had high similarity to fat tissue with difference of 0.03 (dB cm^{-1} MHz^{-1}) and 0.07 (10^6 kg m^{-2} s^{-1}), while B was close to the glandular tissue with difference of 9.2 m s^{-1}. Multilayer breast phantom images' results showed gray levels in mammography and ultrasound modalities. This study succeeded in establishing TMP material for mammography and ultrasound. It can also be used for simple quality assurance and control programs.

Introduction

Mammography is the gold method for breast cancer screening, but it has limited sensitivity for detecting lesions in women with dense breast tissue [1]. Meanwhile, ultrasound imaging can distinguish between cysts and solid masses, thereby reducing unnecessary biopsy procedures [2, 3]. The combination of these two methods can produce imaging modalities with excellent properties. It is also believed to improve the screening evaluation as well as diagnosis of breast cancer. Several studies have also been carried out on the combination of two or more imaging modalities. Moro et al., 2020 [4] combined Magnetic Resonance Imaging (MRI) and ultrasonography (US) images to improve cervical cancer assessment. Emons et al. 2018 [5] also developed a prototype of a combination between mammography and US images to improve breast cancer detection. Berg et al. 2004 [6] compared the evaluation of breast images from clinical examination using US, mammography, MRI, as well as multimodal and single modality. Furthermore, the result showed that more accurate detection results were obtained using multimodal diagnosis.

The development of a tissue-mimicking phantom (TMP) study is important and challenging due to the importance of multimodality imaging. TMP can be used to assess image quality qualitatively and quantitatively. In mammography and US imaging, it must have an X-ray attenuation coefficient that is equivalent to that of the tissue being imitated [7]. Acoustic properties, such as speed of sound, impedance, and attenuation coefficient must be equivalent to that of the imitated water or tissue [8]. The speed of sound (SoS) and attenuation values recommended by the American Institute of Ultrasound in Medicine (AIUM) are 1540 m s^{-1} and 0.3–0.7 (dB cm^{-1} MHz^{-1}) [9]. TMP was also recommended to have

elasticity, hardness, and Poisson's ratio properties, which are equivalent to the physical parameters of human tissue [10].

TMP materials generally consist of biopolymers and polymers obtained from chemical synthesis. Commercial breast phantoms are available in the market, but they are still limited to a single modality. Several studies have been carried out on the development of TMP materials for multimodalities, such as Gelatin + agar for phantom Positron Emission Tomography (PET), B-Mode US, and elastography [11]. Gelatin + psyllium powder has also been used for US and MRI applications [12], while Polyvinyl Alcohol (PVA) was utilized for US and microwave imaging [13]. However, TMP PVA, agar, and Gelatin could not be used repeatedly due to water evaporation and bacterial growth activity. Gelatin and agar materials had poor elastic properties, which makes them unsuitable for mammography imaging.

An alternative TMP material to overcome these problems is Polyvinyl Chloride (PVC). It is a general synthetic polymer that is easy to synthesize, resistant to bacteria, stable over time, and can be used repeatedly [10]. PVC also has excellent acoustic properties to silicon and PDMS for US imaging. A previous study revealed that the speed of the sound was 1,400 m s^{-1} [14], which is closer to common human soft tissue and greater than that of silicon, namely 1,500–1,600 m s^{-1} [15] and 1,000 m s^{-1} [16]. Several studies have been carried out on TMP with PVC materials for multimodality applications. He et al. [17] have also used this synthetic polymer for computed tomography (CT) and magnetic resonance imaging (MRI) applications. Based on the elasticity and image quality, the results obtained in CT and MRI modalities require improvement by varying the plasticizer composition and additives. A study by He et al., 2019 [18] used PVC material for multimodality breast phantoms. Furthermore, the results showed that the phantom gave a higher lesion detection rate in mammographic modalities compared to US and MRI. TMP studies for multimodality phantoms only focused on image results and their mechanical parameter. There was also no comprehensive evaluation of tissue equivalence based on X-ray attenuation properties, especially mammography, as well as acoustic properties in the US.

This study focuses on PVC material as a TMP for dual modalities, namely mammography and US, which were evaluated using mechanical parameters, X-ray attenuation, and US acoustic properties, including SoS, attenuation, and impedance. The quality of simple breast phantom images, such as adipose tissue, glandular tissue, and lesions was also investigated. As new imaging techniques and educational tools are developed, this study becomes essential for cost and time-saving quality assurance, as well as control programs in mammography and the US.

Materials And Method

Design and Fabrication of Polyvinyl Chloride as TMP

The sample case was a box with an area of 10 × 10 cm^2 and a thickness of 1 cm. It was produced from Polylactic Acid (PLA) filament using Creality Ender 5 Plus 3D printing (Shenzhen Creality 3D Technology Co., Ltd). Furthermore, TMM was made of polyvinyl chloride (PVC) material and dioctyl terephthalate

(DOP) plasticizer with the addition of graphite additives and silicon oil. Determination of the composition of PVC and DOP was carried out based on the ratio of the mass percentage to the total mass of 200 g, as shown in Table 1. Compositions A – F were prepared by mixing the raw materials in a beaker, followed by constant stirring at 350 rpm and 180°C. At this temperature, the DOP plasticizer diffused into the PVC particles, followed by stirring to produce a homogeneous matrix characterized by a transparent appearance [19]. After the mixture was cooled to 50°C, it was poured into the PLA case and cooled to room temperature. The sample fabrication results are presented in Fig. 1(a).

Table 1
Composition of PVC-based TMP samples used for measurements of density, elasticity, X-ray attenuation, and ultrasound acoustic properties

TMP sample	PVC (%)	DOP (%)	Graphite (%)	silicone oil (%)
A	5	95	-	-
B	7	93	-	-
C	10	90	-	-
D	20	80	-	-
E	7	90	3	-
F	7	90	-	3

Design and Fabrication of a Breast Phantom for Dual Modality

The breast phantom was box-shaped with a cross-sectional area of 10 × 10 cm^2 and a thickness of 8 cm. It also consists of two layers, namely the bottom glandular mimicking layer and the top adipose layer. There were characteristic lesions (anomalies) in the form of cylinders between the two layers. Fat and glandular tissue mimicking were made from the composition of TMP A and B samples. Meanwhile, a mixture of gypsum and water in a ratio of 2:1 was used to produce the lesion material. The fabricated breast phantom was made in different layers. The lesion was then inserted into the phantom after the underlayer/glandular creation. It was then coated again with a sample of fat-mimicking material. The results of the fabrication are presented in Fig. 1b.

Measurement of Density

The mass density was determined by calculating the mass-to-volume ratio in units (g cm^{-3}). Furthermore, the sample mass was measured using an electronic digital vernier balance, and the volume was verified with the fluid transfer method.

Measurement of the Linear Attenuation Coefficient

The TMP sample's linear attenuation coefficient was calculated using Lambert Beer's Law by referring to image data with and without objects. Acquisition of image data was carried out using a mammography

X-ray machine from 23–35 kV. The parameters used include a current of 40 mAs per unit time; Mo/Mo filters, gantry angle of 0°; no compression; and a distance from the source to the object of 65 cm. The image digitization process uses a gray level value with a window level (WL) of 20 and width (WW) of 7. The results were then saved in the DICOM format (.dcm). The calculation of the linear attenuation coefficient (μ) was carried out using Eq. (1).

$$\mu = \frac{1}{x} \ln \left(\frac{I_0}{I} \right) (1)$$

I_0 is the pixel value obtained from the image without the presence of phantoms or objects, and x is the sample thickness (cm). I is the pixel value obtained from the phantom region image [20, 21].

Measurement of Ultrasound Acoustic Properties

Measurement of the acoustic properties was performed using an acoustic device developed by the Medical Instrumentation Laboratory, Department of Engineering Physics, Institut Teknologi Bandung. This device consists of an Un0rick board, Raspberry Pi, an Ethernet hub, a monitor, and a transducer. This system used the pyUn0.py programming, and the raw data was the change in signal amplitude with time. The settings measurement is presented in Fig. 2.

The speed of sound propagation was tested with the pulse-echo method, where the transducer was used as a receiver and transmitter. There was an ultrasonic gel for sample impedance matching between the transducer and sample, hence, signals are sent and a match is received from the pulser/receiver device. The time between peaks was used to determine the speed of sound and was calculated using Eq. (2).

$$v = 2d \bullet \Delta t \, (2)$$

Where d is the distance traveled by the sound wave ($2d$) (m), v is the speed of sound m s^{-1}, and Δt is the calculated time difference between two consecutive echo peaks. Furthermore, the determination of sample thickness must be considered properly [22]. The result of multiplying the speed of sound by the density is the acoustic impedance (Z) with a unit (10^6 kg m^{-2} s^{-1}) [23].

The acoustic attenuation coefficient was calculated based on the decrease in signal amplitude. The results also showed that the amplitude of the signal reaching the receiving transducer decreases exponentially, and Eq. (3) was used to calculate the attenuation coefficient [22].

$$A = A_0 e^{-\sigma x} \, (3)$$

where A is the amplitude of the echo signal (mV), A_0 is the amplitude of the pulsed signal (mV), σ is the attenuation coefficient (dB cm^{-1} MHz^{-1}), and x is the sample thickness (cm).

Evaluation of Contrast Noise to Ratio of Breast Phantoms for Dual Modality

CNR was calculated with images from inhomogeneous breast phantoms using (4) [23].

$$CNR = \frac{\left|\bar{c}_{in} - \bar{c}_{out}\right|}{\sqrt{\alpha_{in}^2 + \alpha_{out}^2}} (4)$$

where $\bar{c}_{in}$ and $\bar{c}_{out}$ are the average pixel values of the lesion and breast tissue images. α_{in} and α_{out} are the standard deviations for the same region.

Results

Mass Density of TMP

Density values can be used as an inspiration or initial base for assessing the sample, which has the same attenuation properties as the interaction of ionizing radiation in human tissue. The density was used to determine the equivalence of the tissue mimicking the interaction of non-ionizing radiation through the parameter of the acoustic impedance property (on ultrasound). The results of calculating the density of TMP samples made from PVC with a DOP plasticizer are presented in Table 2. In this study, the values of the samples ranged from 0.961 ± 0.012 (sample A) to 1.187 ± 0.035 (g cm^{-3}). The results showed that the concentration of PVC increased along with the density of the tissue-mimicking phantom (TMP).

Table 2
The density value of TMP with variations in PVC composition

Sample	Density (g cm^{-3})
A	0.961 ± 0.012
B	1.001 ± 0.005
C	1.114 ± 0.087
D	1.187 ± 0.035
E	1.063 ± 0.042
F	0.998 ± 0.027
Fat*	0.950
Breast*	1.020
Muscle*	1.050
Soft tissue*	1.043
*from reference [24]	

Linear Attenuation Coefficient of TMP

Figure 3 shows the value of the X-ray linear attenuation coefficient for TMP samples made from PVC with a DOP plasticizer. Measurements were carried out by referring to image data in the range of 23–35 kV using a mammography tube. The results showed that the X-ray attenuation level decreased with increasing X-ray energy. This finding indicates that more X-rays were transmitted than absorbed. The attenuation measurements of these TMP samples were compared with those of a commercial breast ACR phantom (www.phantoms.artinis.com/pasmam-constancy). At a voltage of 23 kV, the value obtained for all samples was greater than that of the phantom. Meanwhile, at a voltage of 28–35 kV, all TMP, except sample D have values close to those of commercial breast ACR. The ratio of the difference in the attenuation coefficient for all tube voltage ranges from the TMP samples is presented in Table 2.

Table 3
The ratio of TMP sample attenuation difference vs. ACR phantom

Voltage (kV)	samples					
	A	B	C	D	E	F
23	0.33	0.51	0.74	1.08	0.67	0.16
28	0.02	0.09	0.25	0.29	0.02	0.01
32	0.37	0.27	0.12	0.62	0.11	0.46
35	1.17	1.33	1.86	4.09	1.39	0.40

From Table 3, the attenuation values of the TMP samples that were close to the ACR breast phantom were F, A, B, E, C, and D. Furthermore, they were evaluated for their acoustic properties at ultrasound working frequency for an assessment study of tissue-mimicking breast phantom dual-modality.

Ultrasound Acoustic Properties of TMP

Figure 4(a) shows the results of measuring the speed of sound (SoS) as a group velocity of ultrasound pulses for seven materials at a frequency function of 1–5 MHz. The SoS value indicated the experimental uncertainty of the frequency function that tends to be linear and constant. This occurred because the pulse's shape can change as it passes through the material of a TMP sample. Furthermore, the SoS values measured in the TMP samples experienced an increase after the addition of PVC concentrations. For example, at 1 MHz, the values ranged from 1536.6 ± 45.6 to 2021.2 ± 17.2 m s^{-1}. The addition of PVC can increase the density, which is proportional to SoS. These findings are in line with Chen et al. 2022 [25], who also obtained similar results. The SoS value increased proportionally with the concentration of the material at the same frequency. The addition of a silicone oil dissolving agent (sample F) did not affect the obtained, but the graphite scattering agent had a major influence.

Figure 4(b) shows the acoustic impedance (Z) values for each TMP sample with a frequency function. The results show that Z also has a dependence that tends to be linear and constant. Furthermore, its value increased along with the concentration of PVC. The PVC with a 5–20% concentration ranged from 1.47 ± 0.003 to 2.39 ± 0.021 (10^6 kg m^{-2} s^{-1}). The results of this Z measurement have a value close to that of Spirou 2005 et al. [26], namely 1.40 ± 6 (10^6 kg m^{-2} s^{-1}).

Figure 5 shows the acoustic attenuation of a TMP sample made of PVC with a variation of DOP plasticizer and additives with a frequency function of 1–5 MHz. The acoustic attenuation coefficients for all PVC samples ranged from 0.51 ± 0.02 to 2.07 ± 0.03 (dB cm^{-1}), at a 1–5 MHz frequency. The values also increased along with the concentration of polyvinyl chloride, and similar results were obtained by Chen et al. 2022 [25]. In this study, the attenuation coefficient of PVC with various concentrations was 1.25 ± 0.162 to 2.07 ± 0.03 dB/cm at a frequency of 5 MHz. These results are consistent with De Carvalho et al. 2016 [27] that the values obtained with an increase in graphite concentration ranged from 0.37 ± 0.01 to 0.61 ± 0.02 (dB cm^{-1} MHz^{-N}). The acoustic attenuation is concentration-dependent. Furthermore, it refers to the loss of mechanical to heat energy due to the thermoviscos effect as well as a function of depth. Based on previous studies, this coefficient is also frequency dependent and expressed as (dB cm^{-1} MHz^{-1}). This relationship had been explained by Mischi et al 2014 [28] that the frequency-dependent attenuation coefficient was expressed as $\alpha_{dB} zf = 10\log_{10}(I/I_t)$. This shows that the attenuation was related linearly and squarely to the frequency. A 2nd order polynomial fitting function was applied to the acoustic attenuation curve in each TMP sample. This choice was based on the attenuation of water that was suitable using a 2nd order polynomial fitting. In some sample materials, the TMP showed that the attenuation no longer changes linearly, but to a quadratic function for higher frequencies.

Table 4
Acoustic properties of human tissue and tissue-mimicking phantom at 1 MHz frequency at room temperature

	Materials	Speed of Sound (m s^{-1})	Attenuation (dB cm^{-1} MHz^{-1})	Acoustic Impedance (10^6 kg m^{-2} s^{-1})
TMP	A	1536.6 ± 45.6	0.51 ± 0.02	1.47 ± 0.003
	B	1556.2 ± 64.0	0.64 ± 0.10	1.55 ± 0.035
	C	1724.6 ± 55.2	0.63 ± 0.17	1.92 ± 0.054
	D	2021.2 ± 17.2	0.63 ± 0.20	2.39 ± 0.021
	E	1907.2 ± 34.4	0.58 ± 0.11	2.02 ± 0.033
	F	1546.2 ± 34.2	0.55 ± 0.12	1.64 ± 0.013
	Zerdine#	1529.9 ± 2.86	0.54 ± 0.02	1.4999
	Agar#	1606.78 ± 13	0.60 ± 0.05	1.696
	PVA 10%‡	1556 ± 26	0.09 ± 0.02	-
	PVA + Sucrose 50%§	1819.2 ± 3.9	0.53 ± 0.03	2.415
Human tissue	Fat	1478	0.48	1.4
	Glandular[α]	1553 ± 35	-	-
		1547 ± 12.1	0.68 ± 0.13 (4.5 MHz)	-
	Skin[β]	1540	9.2 ± 2.2 (5 MHz)	1.71–1.83
	Breast[γ]	1510	0.75	1.54
	Soft tissue[δ]	1561	0.54	1.63
	Tendon[ζ]	1670	4.7	1.84

#: [22]
‡: [29]
§: [30]
: [31, 32]
α: [33, 34]
β: [35]
γ: [36]
δ: [31]
ζ: [24]

Based on the evaluation of mass density properties, X-ray attenuation coefficient, as well as acoustics, samples A and B were used as fat and glandular tissue, which mimicked dual-modality breast phantoms (mammography and ultrasound). From the study of X-rays and sound waves, both of them were close to adipose and glandular tissue. Construction of a box-shaped breast phantom was carried out with a three-layer arrangement and the lesion was then inserted. The bottom to top layer consisted of samples B, A, and B with the insertion of interlayer lesions. The results of dual-modality breast phantom imaging (mammography and ultrasound) are presented in Fig. 6.

Figure 6(a) shows the results of breast phantom images that can be formed in mammography modality with an average gray level of 603.40 ± 62.51 at 35 kV. The cylindrical shape of the lesion can be distinguished clearly in the gypsum material, which provided higher contrast than PMMA. The gray-level glandular and fat tissue gave good results even though air bubbles were still formed. Meanwhile, Fig. 6(b) shows the image of the breast phantom in the ultrasound. The cylindrical shape of the lesion was only clearly visible on the gypsum material, and PMMA obtained a dark color. The second layer obtained a dark color because sample A did not scatter sound waves, hence, a scattering agent was needed. The average gray level and standard deviation obtained from the ultrasound images of the top, middle, and bottom layers were 79.48 ± 20.7, 6.72 ± 1.1, and 26.55 ± 2.16, respectively. Matheo et al. 2018 [37] revealed that the gray level of lactiferous duct, fat, and glandular tissues were 10.18 ± 3.31, 48.41 ± 6.75, and 102.92 ± 11.90, respectively [37]. This study has successfully fabricated a tissue-mimicking of the lactiferous duct and fatty tissue based on the literature data, the glandular part still needs improvement.

Furthermore, CNR evaluation of gypsum cylinder lesions and PMMA in mammographic modalities gave values of 7.27 and 3.90, respectively. In the ultrasound modality, the CNR for gypsum lesions near the surface and at the bottom were 9.37 and 21.19, respectively. It was significant because the mass density properties, X-ray attenuation, acoustic ultrasound, and image phantom can provide promising potential for development as a dual phantom – modality in mammography and ultrasound.

Discussion

PVC-Plasticizer DOP material as TMP for mammography and ultrasound dual-modality breast phantom has been evaluated using parameters of density, elasticity, x-ray attenuation, SoS, acoustic attenuation, impedance, and image. From Table 1, the density of the sample had close tissue equivalent to that of humans. For example, samples A and F were close to fat tissue with a difference of 1.16%. Meanwhile, B and F were close to the breast with a difference of 1.9 and 2.2%, respectively. Samples C, D, and E have good equivalence with the muscle tissues [24]. Based on a previous study, the density obtained was also similar to that of Jeong et al. 2017 [38], where a value of 1.02 (g cm^{-3}) was obtained for PVC-Plasticizer in phantom ultrasound applications. The difference in these values was due to the various concentration levels of PVC. A sample density equivalent to human tissue is the base element for estimating X-ray attenuation properties (mammography), SoS, and acoustic impedance. TMP density close to tissue can have close tissue equivalent to X-ray and ultrasound properties.

Meanwhile, Fig. 3 shows the linear attenuation coefficients of the X-ray samples that were compared with commercial breast ACR phantoms. The results between samples A, B, C, E, F, and the ACR phantoms gave promising results at 28–35 kV. However, for low voltages, the results were relatively different. From the literature data obtained by Heine et al. 2006 [39], the average X-ray linear attenuation coefficient of all samples has a difference of 1.29 ± 0.25 from that of the 50%-50% glandular-fat tissue [39]. This difference was due to variations in the quality of the X-ray tube from each manufacturer of mammography modalities. Samples A, B, C, E, and F have a close tissue equivalent with the X-ray attenuation properties of the ACR phantom. The value of the linear attenuation coefficient with a voltage obtained a quadratic relationship with a regression value of 0.957 as well as a t-test with a p-value of 0.431, which was greater compared to the set α-value of 0.05. This indicates that the fitting data does not show a significant difference with a regression value of 0.95. These results are consistent with Sato et al.2021 that the linear attenuation coefficient provides a non-linear relationship with X-ray energy [40].

Figures 4(a) and (b) show that SoS and Z obtained a trend of a constant-linear relationship to the frequency variation of 1–5 MHz with an average linear regression fitting of 0.643 for SoS and 0.675 for Z. Based on the t-test, the SoS and Z regression values obtained p-values of 0.027 and 0.036, respectively, which were smaller compared to the set α-value of 0.05. This indicates that the two data fitting results show a significant difference with a regression value of 0.95. Furthermore, the SoS and Z data do not show a linear response with frequency. These results are in line with Zell et al. 2007 [41] who stated that SoS has a very linear and constant dependence. The σ data showed a quadratic response to frequency variations with an average regression value of 0.978 and obtained a p-value equal to the set α-value of 0.05. The regression results were closer to the value of 1, indicating that the fitting were more accurate. The acoustic attenuation had an increasing trend as the frequency increased. These findings are similar to that of Villa et al. 2020 and Zell et al. 2007 [30, 41] that the attenuation coefficient increased proportionally with the frequency following the Power Law function.

Figures 4 and 5 compared the acoustic parameter measurements with human tissue data literature and other materials tissue-mimicking phantom as benchmarking, which were summarized in Table 4. The selection of this literature refers to the suitability of the frequency range used in the study. Based on SoS parameters, samples A, B, and F had close tissue equivalent to glandular with a difference of -10.4, 3.2, and − 0.8 m s^{-1}, respectively. The SoS of samples A, B, and F also have good equivalence with breast, soft tissue, and skin. The results also showed that D and E refer to stiff samples, such as trabecular bone at 1,886 m s^{-1} [42]. When referring to the parameters of attenuation and acoustic impedance, sample A had an excellent equivalence to fat tissue with a difference of 0.03 (dB cm^{-1} MHz^{-1}) and 0.07 (10^6 kg m^{-2} s^{-1}), respectively. Sample B also was close to glandular tissue by referring to SoS values and acoustic attenuation. However, the acoustic attenuation parameter still requires further study. Sample A had an excellent close equivalence with the commercial phantom material Zerdine with a difference of 6.7 m s^{-1}, -0.03 (dB cm^{-1} MHz^{-1}), and − 0.03 (10^6 kg m^{-2} s^{-1}), respectively. The composition of the PVC-plasticizer material with agar and PVA materials competed with several studies' results, which are summarized in Table 4.

The difference between TMP samples and human tissue can be caused by several factors, such as the molecular weight of the PVC-Plasticizer, which was low or exceeded during fabrication, thereby affecting X-ray attenuation and SoS, or requiring a scattering agent to increase the acoustic attenuation. Achieving tissue equivalence that satisfies both X-ray and ultrasonic waves is relatively challenging. However, the proposed TMP results were close to breast tissue, including A and B. This indicates that they satisfied the requirements as breast phantom material for dual-modality (mammography and ultrasound).

Figure 6 shows breast phantom images from samples A and B with lesions inserted for quality assurance and control. Cylindrical insertion lesions were both seen on mammography and ultrasound modalities. The gray level of breast tissue in the mammography modality obtained results that followed the breast ACR phantom. However, the ultrasound modality on layer A (PVC5%) obtained a gray level close to black. This was due to the lack of a scattering agent to increase the speckle of the ultrasound image. The adipose tissue pulse SoS factor was 1.27% lower than that of glandular tissue. This caused the contribution of the refractive effect to be small for the fat-to-glandular interface, hence, the pulse group's speed difference did not produce artifacts in the image. These findings are consistent with Carvalho et al. [27], where similar results were recorded. The results obtained have provided an important aspect in developing multimodal phantoms. This material has several other advantages, such as low-cost and reusability [37]. Improvements that can be carried out include adding scatter agents and completeness features to perform quality assurance as well as control of mammography and ultrasound modalities.

Conclusion

This study revealed the potential of polyvinyl chloride (PVC) material with the ratio of plasticizer addition for dual-modality breast phantom tissue in mammography and ultrasound. Promising results were obtained that PVC-Plasticizer material, including samples A, B, and F had properties close to adipose, glandular, and lactiferous duct tissues based on density parameters, X-ray linear attenuation coefficient with a difference of 0.26–0.55 from the ACR phantom, SoS below 1,600 m s^{-1}, attenuation at 0.51–0.64 dB cm^{-1} MHz^{-1}, and acoustic impedance of 1.47–1.64 106 kg m^{-2} s^{-1}. This study succeeded in establishing a generalized breast phantom for quality assurance in mammography and ultrasound modalities. It is also helpful in training, educating, running controlled quality assurance programs, and developing improved dual-modality imaging techniques.

Declarations

Acknowledgments The authors are grateful to the management of the Gambiran General Hospital, Kediri, Indonesia, and the Medical Instrumentation Laboratory, Engineering Physics Department, Institut Teknologi Bandung, for the permission to conduct this study, as well as to collect and analyze data.

Author contributions Aditya Prayugo Hariyanto prepared and wrote the original draft. Furthermore, Endarko, Freddy Haryanto, Kwan Hoong Ng, and Suprijanto were involved in reviewing/editing the draft. Aditya Prayugo, Endarko, Hariyanto, Freddy Haryanto, and Kwan Hoong Ng performed investigation,

sample preparation, methodology, and visualization. Aditya Prayugo Hariyanto and Nurhanifa Tri Budiarti carried out data collection.

Funding This study was funded by the Institut Teknologi Sepuluh Nopember (ITS) and Kemendikbudristek under Penelitian Disertasi Doktor with reference No. 1393/PKS/ITS/2022.

Conflict of interest: The authors declare that there are no conflicts of interest to disclose.

Ethical approval: This study does not involve human participants or animals.

Informed consent This experiment was carried out on a phantom, and no participation consent was obtained.

References

1. C. Fedon, M. Caballo, R. Longo, A. Trianni, and I. Sechopoulos (2018) Internal breast dosimetry in mammography: Experimental methods and Monte Carlo validation with a monoenergetic x-ray beam. Med. Phys 45(4):1724–1737. https://doi.org/ 10.1002/mp.12792.
2. A. T. Stavros, D. Thickman, C. L. Rapp, M. A. Dennis, S. H. Parker, and G. A. Sisney (1995) Solid breast nodules: use of sonography to distinguish between benign and malignant lesions. Radiology (196)1:123–134. https://doi.org/10.1148/radiology.196.1.7784555.
3. H. M. Zonderland, E. G. Coerkamp, J. Hermans, M. J. van de Vijver, and A. E. van Voorthuisen (1999) Diagnosis of breast cancer: contribution of US as an adjunct to mammography. Radiology 213(2):413–422. https://doi.org/10.1148/radiology.213.2.r99nv05413.
4. F. Moro *et al* (2020) Fusion imaging of ultrasound and MRI in the assessment of locally advanced cervical cancer: a prospective study. Int. J. Gynecol. Cancer 30(4):456 LP – 465. https://doi.org/10.1136/ijgc-2019-000902.
5. J. Emons *et al* (2018) Initial clinical results with a fusion prototype for mammography and three-dimensional ultrasound with a standard mammography system and a standard ultrasound probe. Acta radiol 59(12):1406–1413. https://doi.org/10.1177/0284185118762249.
6. W. A. Berg *et al* (2004) Diagnostic accuracy of mammography, clinical examination, US, and MR imaging in preoperative assessment of breast cancer. Radiology 233(3):830–849. https://doi.org/10.1148/radiol.2333031484.
7. D. R. White (1993) The Design and Manufacture of Anthropomorphic Phantoms. Radiat. Prot. Dosimetry 49(1–3):359–369. https://doi.org/10.1093/rpd/49.1-3.359.
8. Y. Cao, G. Y. Li, X. Zhang, and Y. L. Liu (2017) Tissue-mimicking materials for elastography phantoms: A review. Extrem. Mech. Lett 17:62–70. https://doi.org/10.1016/j.eml.2017.09.009.
9. J. E. Browne, K. V Ramnarine, A. J. Watson, and P. R. Hoskins (2003) Assessment of the acoustic properties of common tissue-mimicking test phantoms. Ultrasound Med. Biol 29(7):1053–1060. https://doi.org/10.1016/S0301-5629(03)00053-X.

10. W. Li *et al* (2016) Polyvinyl chloride as a multimodal tissue-mimicking material with tuned mechanical and medical imaging properties. Med. Phys 43(10):5577–5592. https://doi.org/10.1118/1.4962649.
11. J. Dang *et al* (2011) Development of an anthropomorphic breast phantom for combined PET, B-mode ultrasound and elastographic imaging. IEEE Trans. Nucl. Sci 58(3 PART 1):660–667. https://doi.org/10.1109/TNS.2011.2105279.
12. L. W. Hofstetter *et al* (2020) Development and characterization of a tissue mimicking psyllium husk gelatin phantom for ultrasound and magnetic resonance imaging. Int. J. Hyperth. Off. J. Eur. Soc. Hyperthermic Oncol. North Am. Hyperth. Gr 37(1):283–290. https://doi.org/10.1080/02656736.2020.1739345.
13. M. Usumura *et al* (2021) Longitudinal stability of a multimodal viscoelastic polyacrylamide gel phantom for magnetic resonance and ultrasound shearwave elastography. PLoS One 16(5):1–11. https://doi.org/10.1371/journal.pone.0250667.
14. N. Hungr, J.-A. Long, V. Beix, and J. Troccaz (2012) A realistic deformable prostate phantom for multimodal imaging and needle-insertion procedures. Med. Phys 39(4):2031–2041. https://doi.org/10.1118/1.3692179.
15. H. Tanoue, Y. Hagiwara, K. Kobayashi, and Y. Saijo (2011) Ultrasonic tissue characterization of prostate biopsy tissues by ultrasound speed microscope. Annu. Int. Conf. IEEE Eng. Med. Biol. Soc. IEEE Eng. Med. Biol. Soc. Annu. Int. Conf. 2011(2011):8499–8502. https://doi.org/10.1109/IEMBS.2011.6092097.
16. I. M. De Carvalho, R. L. Q. Basto, A. F. C. Infantosi, M. A. Von Krüger, and W. C. A. Pereira (2010) Breast ultrasound imaging phantom to mimic malign lesion characteristics. Phys. Procedia 3(1):421–426. https://doi.org/10.1016/j.phpro.2010.01.055.
17. Y. He *et al* (2019) Characterizing mechanical and medical imaging properties of polyvinyl chloride-based tissue-mimicking materials. J. Appl. Clin. Med. Phys 20(7):176–183. https://doi.org/10.1002/acm2.12661.
18. Y. He *et al* (2019) 3D-printed breast phantom for multi-purpose and multi-modality imaging. Quant. Imaging Med. Surg 9(1):63–74. https://doi.org/10.21037/qims.2019.01.05.
19. O. Fenollar, L. Sanchez-Nacher, D. Garcia-Sanoguera, J. López, and R. Balart (2009) The effect of the curing time and temperature on final properties of flexible PVC with an epoxidized fatty acid ester as natural-based plasticizer. J. Mater. Sci 44(14):3702–3711: https://doi.org/10.1007/s10853-009-3495-7.
20. D. Ivanov *et al* (2018) Suitability of low density materials for 3D printing of physical breast phantoms. Phys. Med. Biol 63:175020. https://doi.org/10.1088/1361-6560/aad315.
21. B. E. Yunker *et al* (2020) Characterization of 3-Dimensional Printing and Casting Materials for use in Computed Tomography and X-ray Imaging Phantoms. Journal of Research (NIST JRES) 125(125028):1–24. https://doi.org/10.6028/jres.125.029

22. E. Çetin, H. O. Durmuş, B. Karaböce, and N. Kavakli (2019) Acoustical Characterization of Tissue - Mimicking Materials. Med. Meas. Appl. MeMeA 2019 - Symp. Proc:1–5. https://doi.org/10.1109/MeMeA.2019.8802203.
23. F. J. Thomson (2006) Automatic technique parameter selection on a digital mammography system: An evaluation of SNR and CNR as a function of AGD on a GE Senographe DS. Australas. Phys. Eng. Sci. Med 29(3):251–256. https://doi.org/10.1007/BF03178573.
24. M. O. Culjat, D. Goldenberg, P. Tewari, and R. S. Singh (2010) A review of tissue substitutes for ultrasound imaging. Ultrasound Med. Biol 36(6):861–873. https://doi.org/10.1016/j.ultrasmedbio.2010.02.012.
25. P. Chen *et al* (2022) Acoustic characterization of tissue-mimicking materials for ultrasound perfusion imaging research. Ultrasound Med. Biol 48 (1):124–142. https://doi.org/10.1016/j.ultrasmedbio.2021.09.004.
26. G. M. Spirou, A. A. Oraevsky, I. A. Vitkin, and W. M. Whelan (2005) Optical and acoustic properties at 1064 nm of polyvinyl chloride-plastisol for use as a tissue phantom in biomedical optoacoustics. Phys. Med. Biol 50(14):N141-53. https://doi.org/10.1088/0031-9155/50/14/N01.
27. I. M. De Carvalho *et al* (2016) Polyvinyl chloride plastisol breast phantoms for ultrasound imaging. Ultrasonics. 70: 98–106. https://doi.org/10.1016/j.ultras.2016.04.018.
28. M. Mischi, N. G. Rognin, and M. A. Averkiou (2014) Comprehensive Biomedical Physics: Ultrasound Imaging Modalities. Elsevier B.V, vol 2:361-385. https://doi.org/10.1016/B978-0-444-53632-7.00217-3
29. L. Braunstein, S. C. Brüningk, I. Rivens, J. Civale, and G. ter Haar (2022) Characterization of Acoustic, Cavitation, and Thermal Properties of Poly(vinyl alcohol) Hydrogels for Use as Therapeutic Ultrasound Tissue Mimics. Ultrasound Med. Biol 48(6):1095–1109. https://doi.org/10.1016/j.ultrasmedbio.2022.02.007.
30. E. Villa, N. Arteaga-Marrero, J. González-Fernández, and J. Ruiz-Alzola (2020) Bimodal microwave and ultrasound phantoms for non-invasive clinical imaging. Sci. Rep 10(1):1–10. https://doi.org/10.1038/s41598-020-77368-5.
31. T. D. Mast (200) Empirical relationships between acoustic parameters in human soft tissues. Acoust. Res. Lett. Online 1(2000):37–42. https://doi.org/10.1121/1.1336896.
32. X. Gong, Z. Zhu, T. Shi, and J. Huang (1989) Determination of the acoustic nonlinearity parameter in biological media using FAIS and ITD methods. J. Acoust. Soc. Am 86(1):1–5. https://doi.org/10.1121/1.398326.
33. K. T. DUSSIK, D. J. FRITCH, M. KYRIAZIDOU, and R. S. SEAR (1958) Measurements of articular tissues with ultrasound. *Am. J. Phys. Med.* 37(3):160–165. PMID: 13545384
34. E. L. Madsen, J. A. Zagzebski, and G. R. Frank (1982) An anthropomorphic ultrasound breast phantom containing intermediate-sized scatterers. Ultrasound Med. Biol 8(4): 381–392. https://doi.org/10.1016/s0301-5629(82)80006-9.

35. F. A. Duck (1990) Chapter 4 - Acoustic Properties of Tissue at Ultrasonic Frequencies. Academic Press, London, pp. 73–135. https://doi.org/10.1016/B978-0-12-222800-1.50008-5
36. D. E. Collins (1999) ICRU Report 61: Tissue Substitutes, Phantoms And Computational Modelling In Medical Ultrasound. Radiol. Technol 71(215).
37. L. L. De Matheo *et al* (2018) PVCP-based anthropomorphic breast phantoms containing structures similar to lactiferous ducts for ultrasound imaging : A comparison with human breasts. Ultrasonics. 90(November 2017):144–152. https://doi.org/10.1016/j.ultras.2018.06.013.
38. E. ju Jeong *et al* (2017) Fabrication and characterization of PVCP human breast tissue-mimicking phantom for photoacoustic imaging. Biochip J 11(1): 67–75. https://doi.org/10.1007/s13206-016-1109-4.
39. J. J. Heine and M. Behera (2006) Effective x-ray attenuation measurements with full field digital mammography. *Med. Phys* 33(11):4350–4366. https://doi.org/10.1118/1.2356648.
40. K. Sato *et al* (2021) Accuracy of spectral curves at different phantom sizes and iodine concentrations using dual-source dual-energy computed tomography. Phys. Eng. Sci. Med 44(1):103–116. https://doi.org/10.1007/s13246-020-00958-0.
41. K. Zell, J. I. Sperl, M. W. Vogel, R. Niessner, and C. Haisch (2007) Acoustical properties of selected tissue phantom materials for ultrasound imaging. Phys. Med. Biol 52(20). https://doi.org/10.1088/0031-9155/52/20/N02.
42. K. A. Wear (2005) The dependencies of phase velocity and dispersion on trabecular thickness and spacing in trabecular bone-mimicking phantoms. J. Acoust. Soc. Am 118(2): 1186–1192. https://doi.org/10.1121/1.1940448.

Figures

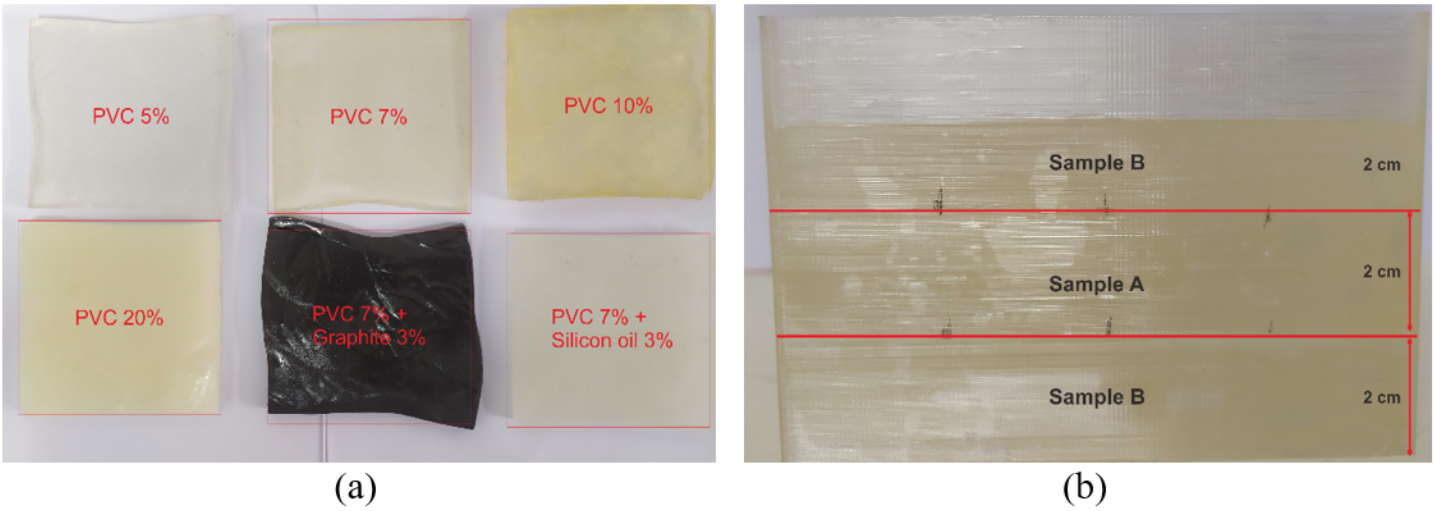

Figure 1

(a) fabrication results of TMP samples made from PVC, (b) PVC breast phantom from the composition of TMP samples A and B with a thickness of 2 cm

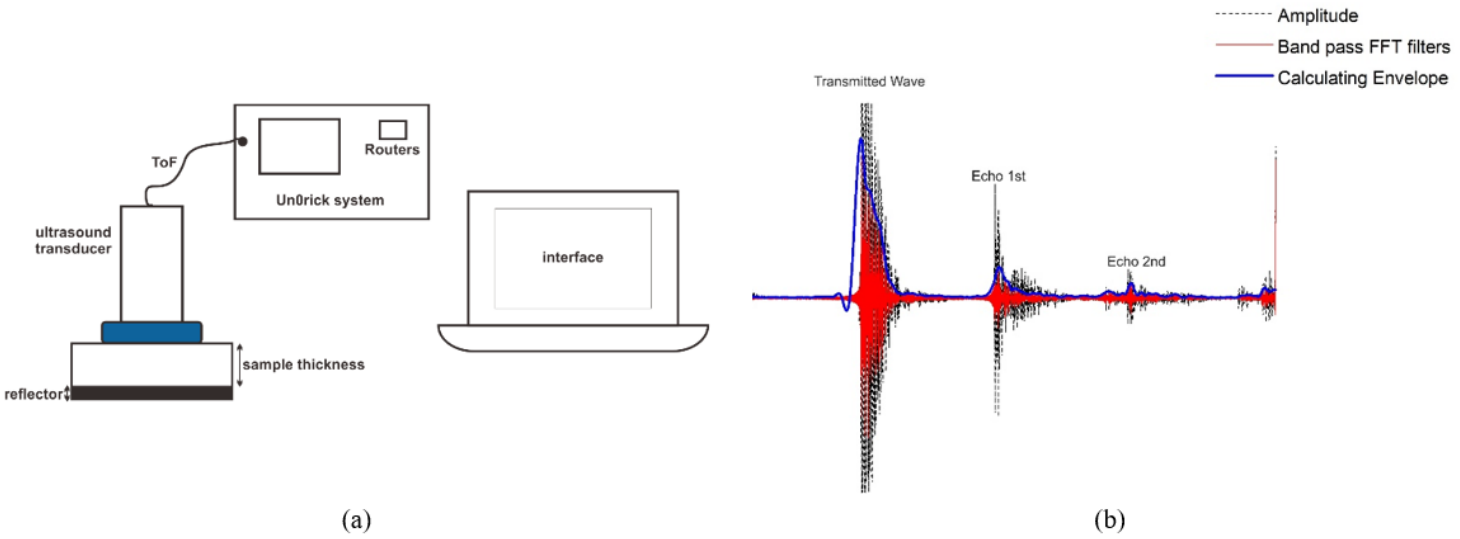

Figure 2

(a) Data collection settings using Un0rick, (b) Observed echo patterns to determine the speed of sound.

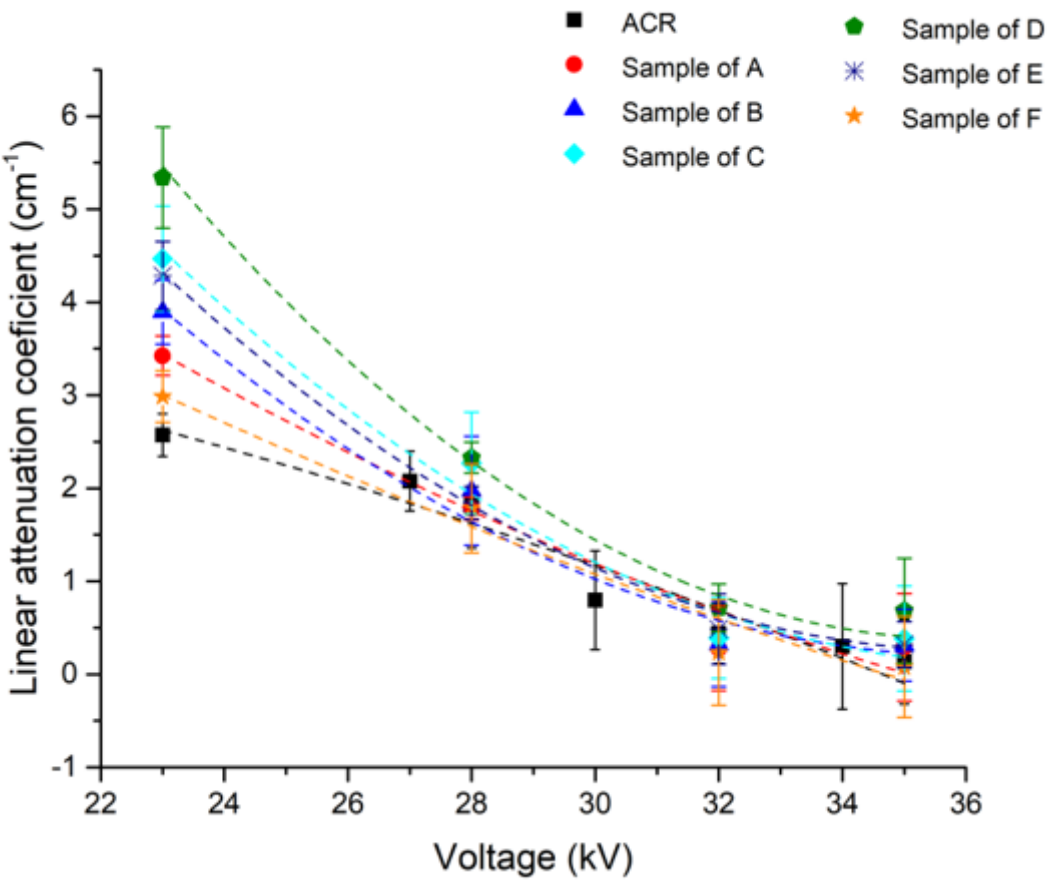

Figure 3

Comparison of the attenuation coefficient values of the TMP and ACR phantom samples

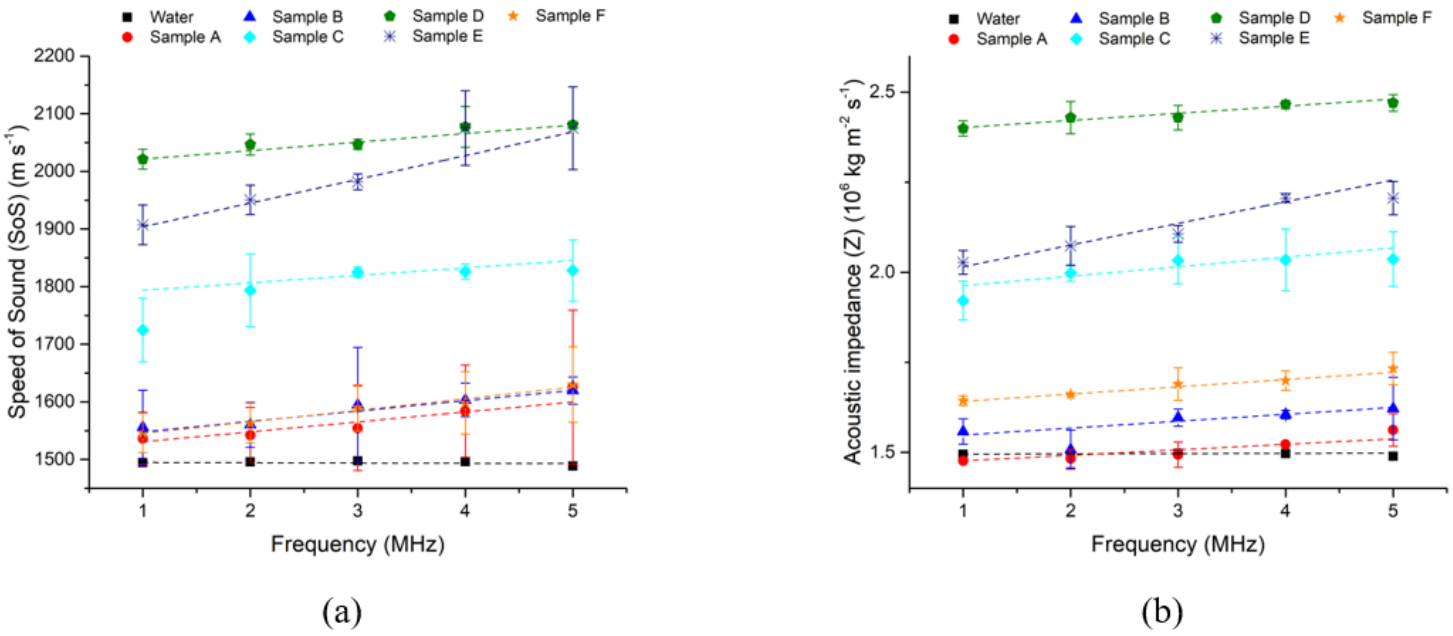

Figure 4

Value of (a) the speed of sound and (b) the acoustic impedance of water and TMP at a frequency of 1 – 5 MHz. (hubungan speed

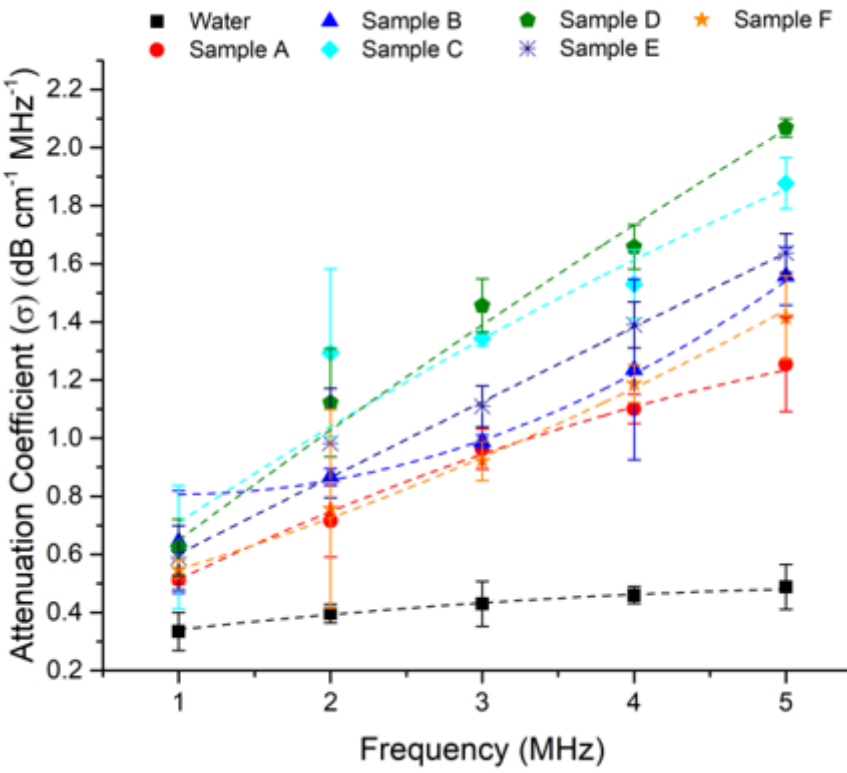

Figure 5

Acoustic attenuation coefficient values of water and TMP at a frequency of 1 – 5 MHz.

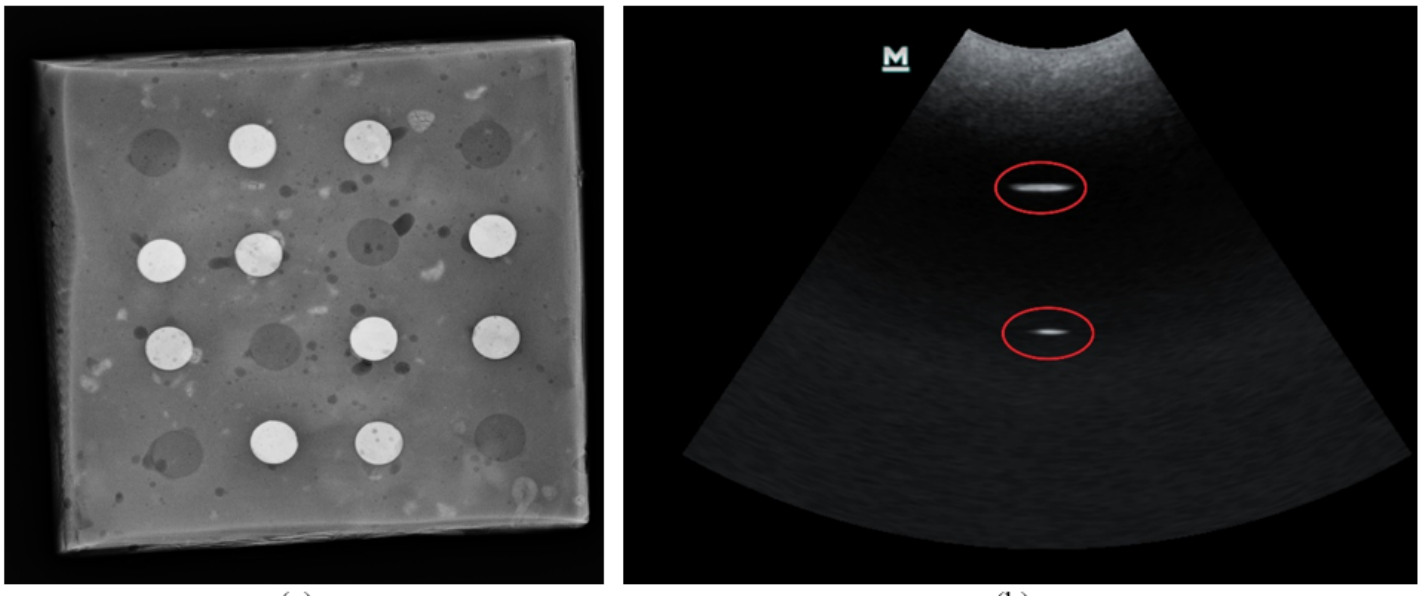

Figure 6

Image of breast phantom dual modality of (a) mammography and (b) ultrasound of PVC-Plasticizer material with features of cylindrical lesions made of calcium and PMMA material